



Fine-Scale Modeling Approaches for Two-Phase Flow

Sanjoy Banerjee
**CUNY Distinguished Professor of Chemical
Engineering**
Director, The CUNY Energy Institute
City College New York,
The City University of New York
email: banerjee@che.ccnycuny.edu
**Collaborators: Frederic Gibou, Jean-Christophe
Nave, Vittorio Badalassi, Djamel Lakehal**

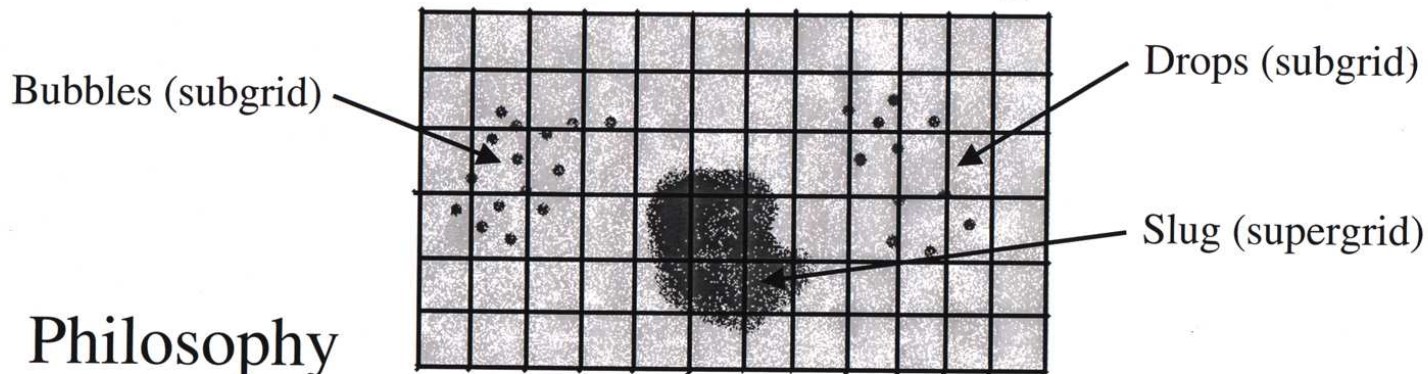
Keynote Lecture, Grenoble, France
September 11, 2008



Main Topics

1. Approaches to fine-scale modeling
2. Interface tracking methods
3. Phase field simulations
4. Level-set and ghost fluid
5. Boundary fitting DNS: physical insights
6. Conclusions

Interface Resolving Methods



- Philosophy

- Resolve supergrid scale structures (VOF, embedded interface, finite elements, level sets)
- Model subgrid scale motion (interpenetrating continua, Euler-Lagrange, homogeneous)

- Advantage

- Subgrid scale motions are more “universal” and hence easier to model (usually dispersed phase)
- Overall problem can be treated as a single fluid with variable density, variable viscosity -- sharp changes at the interface. Reduces needs for closure relationships



Interface Tracking Approaches

1. Phase Field
2. Boundary fitting: low steepness waves
3. Implicit interface tracking:
 4. Level set/ghost fluid
 5. VOF/MARS
6. Explicit tracking/Lagrangian



Why a phase-field approach ?

- Diffuse interface approach facilitates numerical convergence
- Equations of motion for material rather than boundary
- Simulations to realistic length and time scales
- Simple – order parameter distinguishes between fluid material



Semi-Implicit Procedure (Majorization)

- Semi-implicit method using a majorization technique (example for Euler method):

$$\frac{C^{n+1} - C^n}{\Delta t} + \vec{v}^n \cdot \nabla C^n = \frac{1}{Pe} \left[a \nabla^2 \mu^{n+1} + \nabla \cdot \chi^n \nabla \mu^n - a \nabla^2 \mu^n \right]$$

- If $a \geq \frac{1}{2} \max \chi$ the method is unconditionally stable. For the nonlinear term $\psi'(C)$ in $\mu = \beta \psi'(C) - \alpha \nabla^2 C = 0$ we write $\nabla^2 \psi'(C) = \nabla \cdot (\psi'' \nabla C)$ and let $a = \frac{1}{2} \max(\psi''(C)) = \frac{1}{2} \psi''(\pm 1) = 1$
- Result: we remove the fourth and second order time step restrictions!



Model Structure

Order parameter C (conserved form): Model H

$$\frac{\partial C}{\partial t} + \vec{v} \cdot \nabla C = \frac{1}{Pe} \nabla \cdot \lambda \nabla \mu$$

$$Re \left[\frac{\partial \vec{v}}{\partial t} + (\vec{v} \cdot \nabla) \vec{v} \right] = -\vec{\nabla} p + \vec{\nabla} \cdot \left(\vartheta \left(\vec{\nabla} \vec{v} + \vec{\nabla} \vec{v}^T \right) \right) + \frac{1}{Ca} \mu \vec{\nabla} C$$

$\mu = C^3 - C - \nabla^2 C$ is the chemical potential

$$Re = \frac{\rho U_c \xi}{\eta}, \quad Pe = \frac{U_c \xi}{M_c \beta}, \quad Ca = \frac{\alpha \eta U_c}{\beta^2 \xi} = \frac{2 \eta U_c}{3 \sigma}$$



Free Energy: Landau-Ginzburg Form

- Free energy $A[C]$:

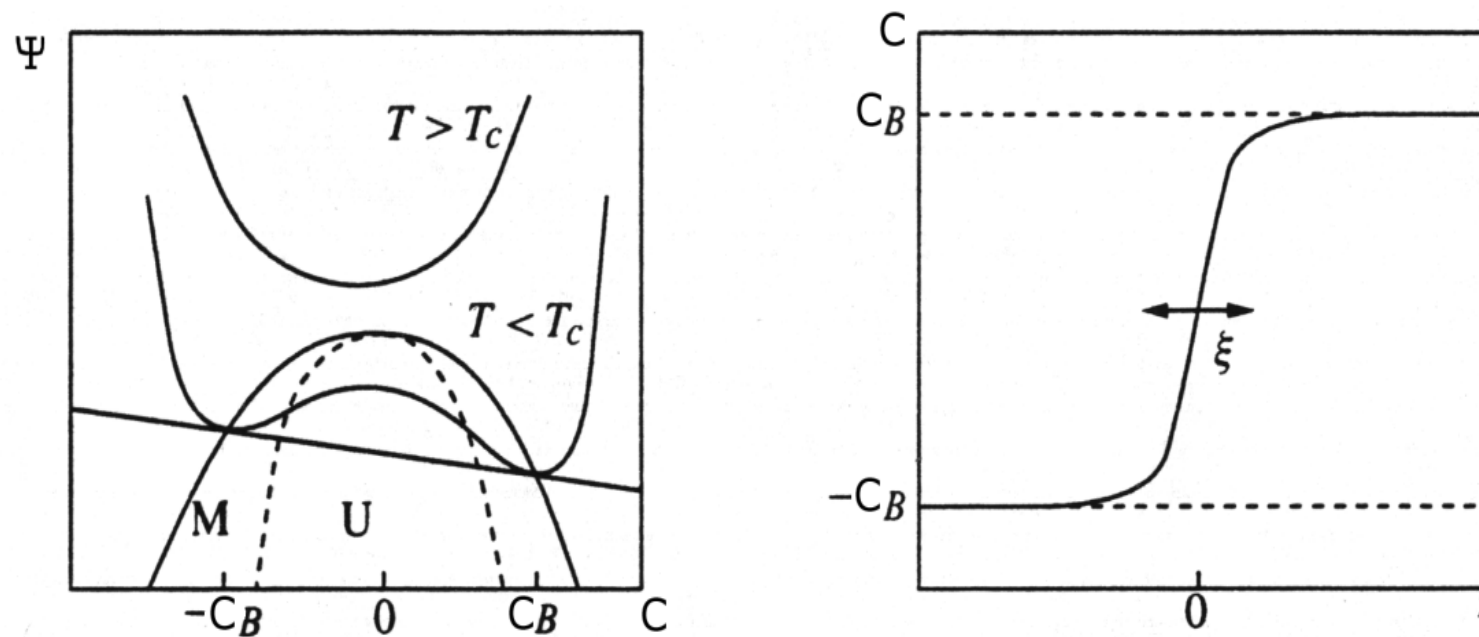
$$A[C] = \int_{\Omega} \left\{ \beta \psi(C) + \frac{1}{2} \alpha |\nabla C|^2 \right\}$$

- At equilibrium the functional $A[C]$ will be a minimum with respect to variations of the function C :

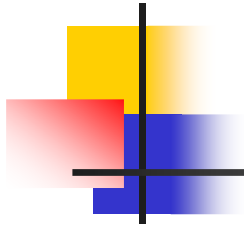
$$\mu = \frac{\delta A}{\delta C} = \beta \psi'(C) - \alpha \nabla^2 C = 0$$

- Surface tension $\sigma \propto \sqrt{\alpha\beta}$, Interface thickness $\xi \propto \sqrt{\alpha/\beta}$
- ψ is the homogeneous free energy (e.g. double well pot.)
- $|\nabla C|^2$ is the gradient free energy

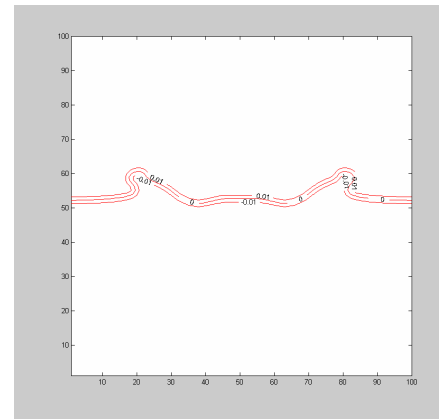
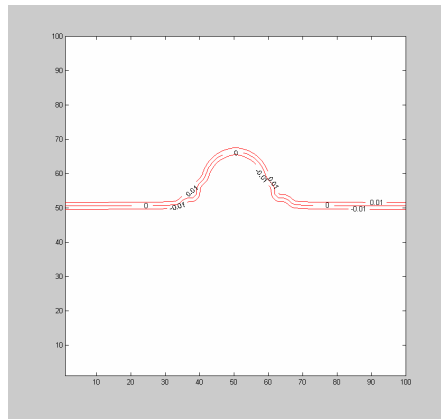
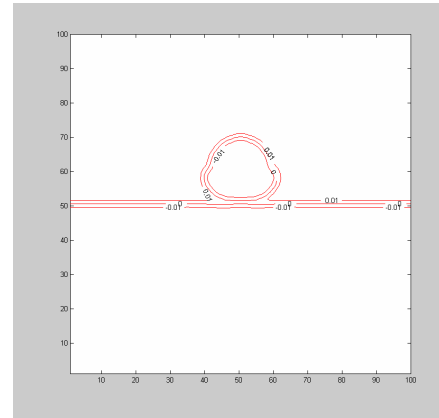
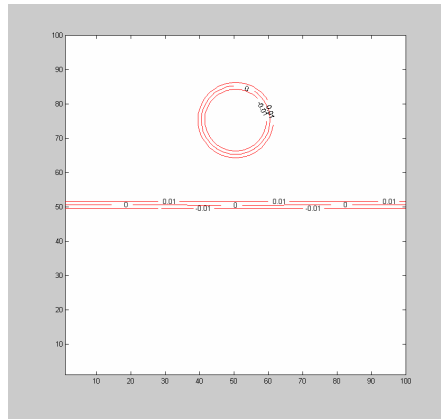
Double-well Potential and Interface Thickness

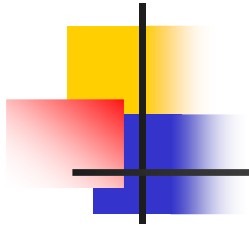


Schematic picture of the homogeneous specific free energy Ψ as a function of C (left) and the equilibrium interface profile (right).

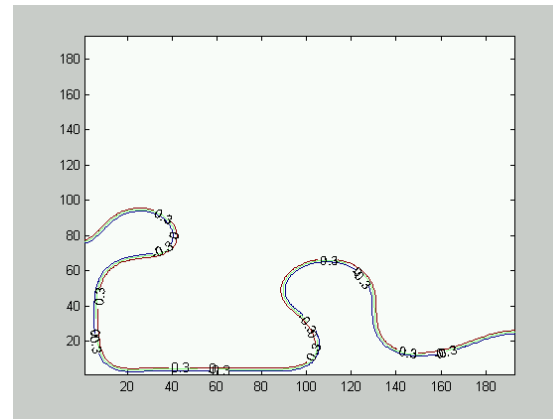
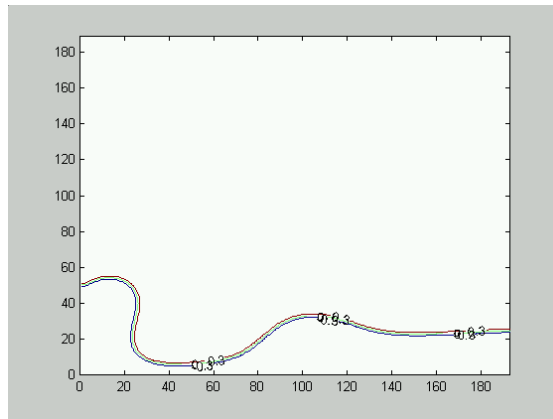
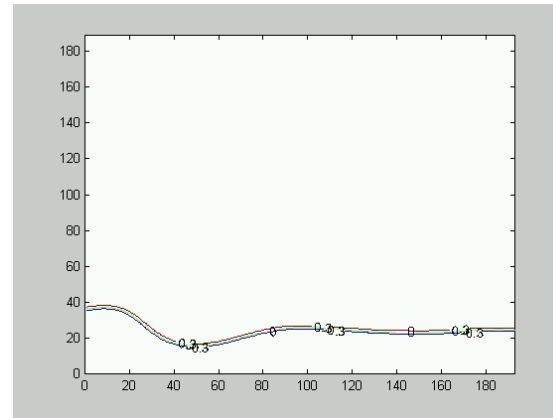
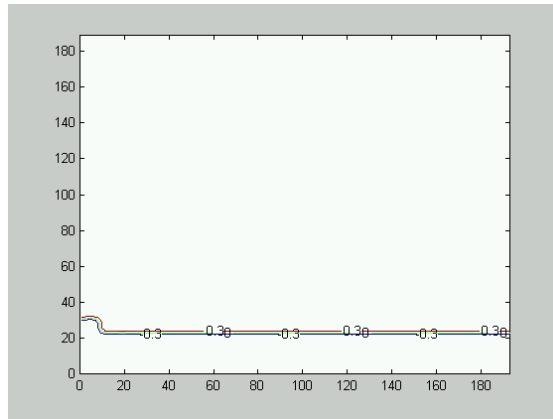


Falling Drop on Free Surface

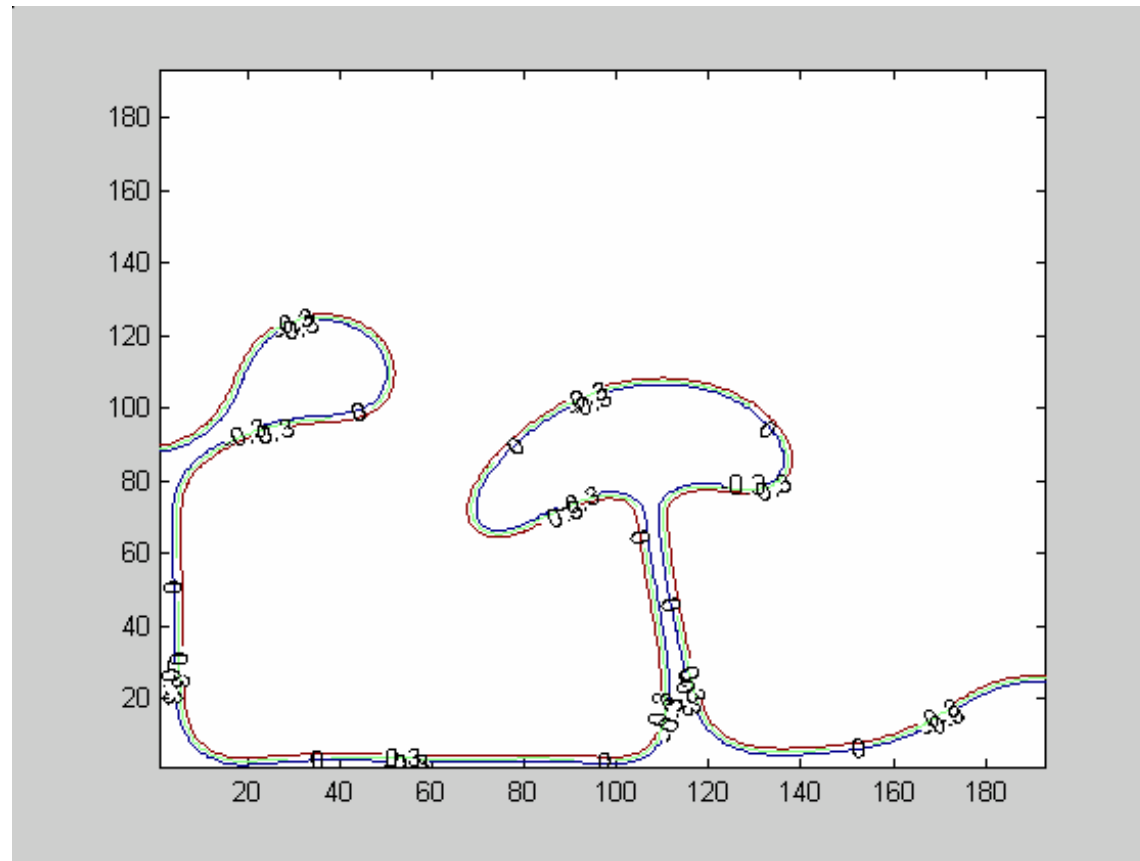


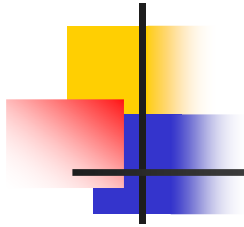


Rayleigh Taylor Instability

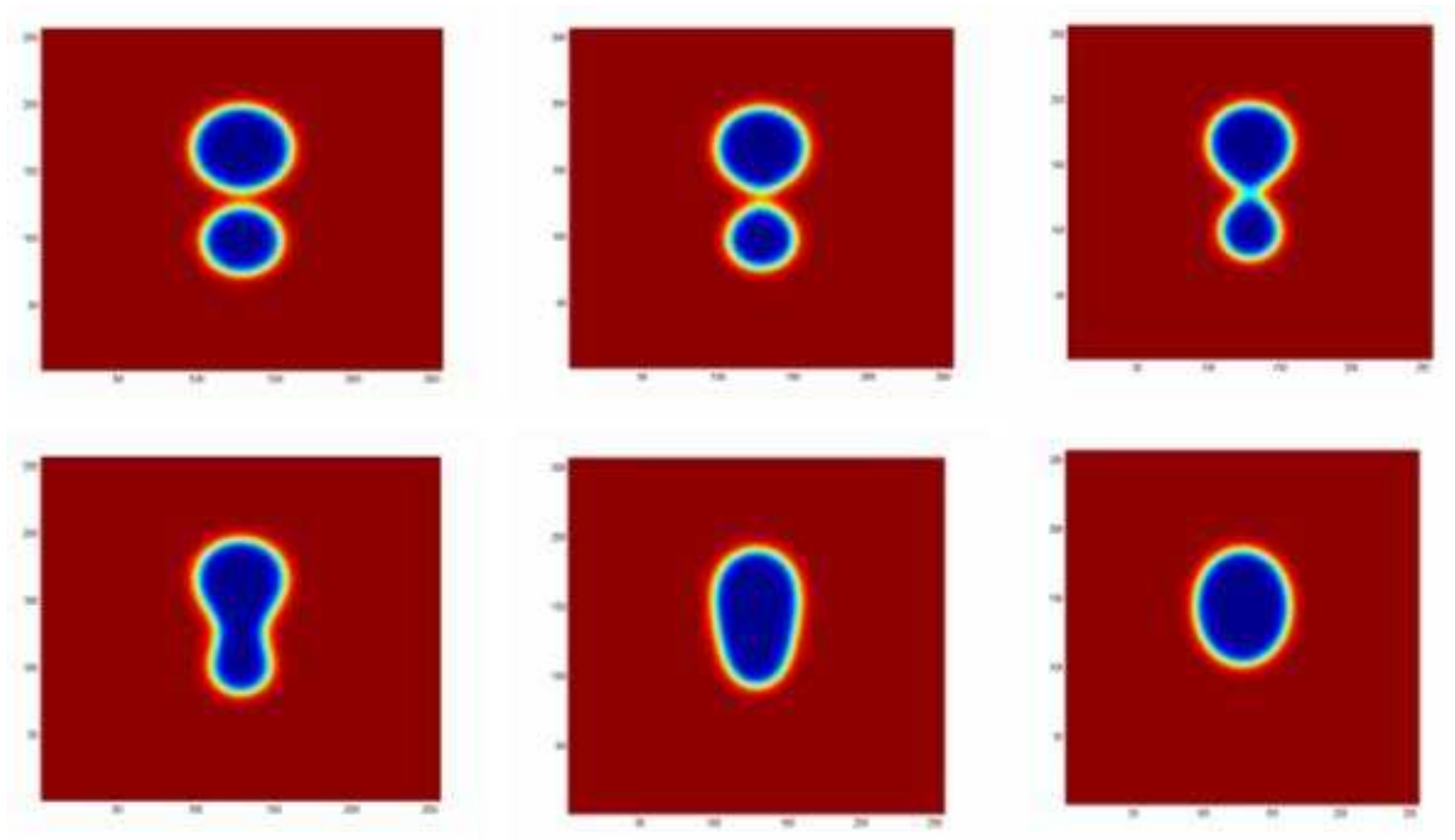


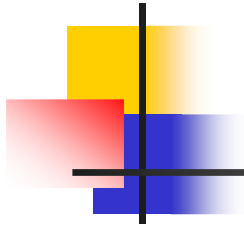
Rayleigh Taylor Instability (Cont'd)





Drop Coalescence

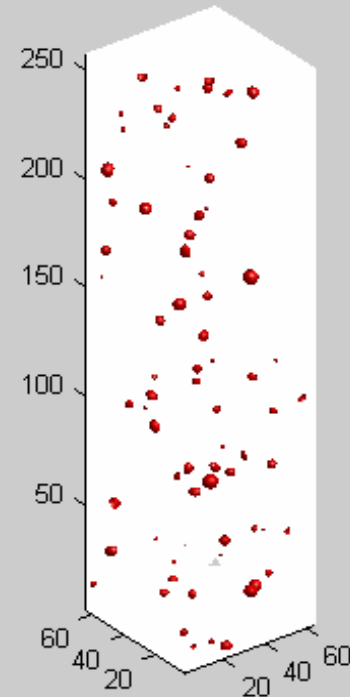
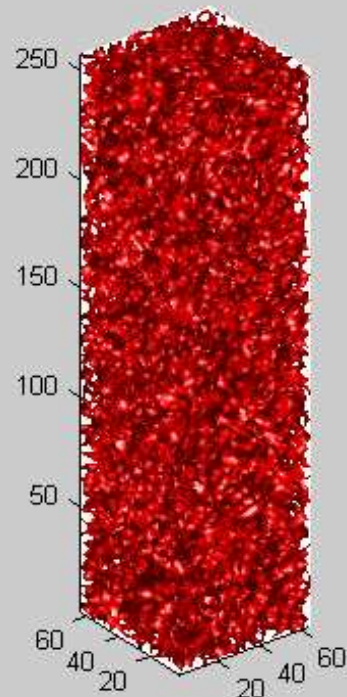




Phase Separation: Density Mismatch

Critical (50/50)

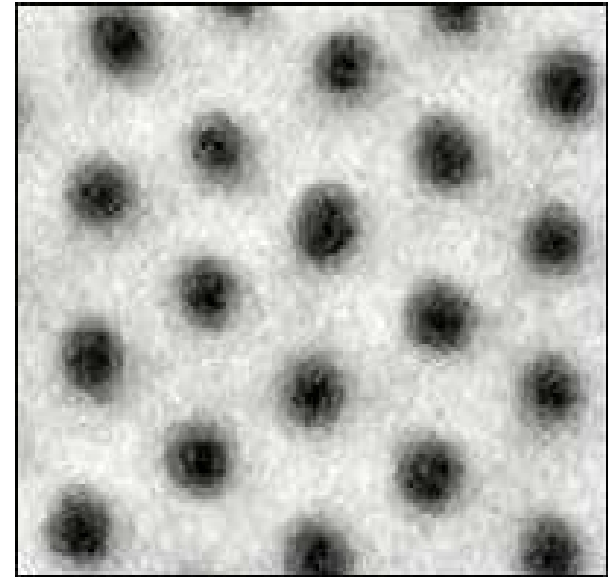
Not Critical (20/80)



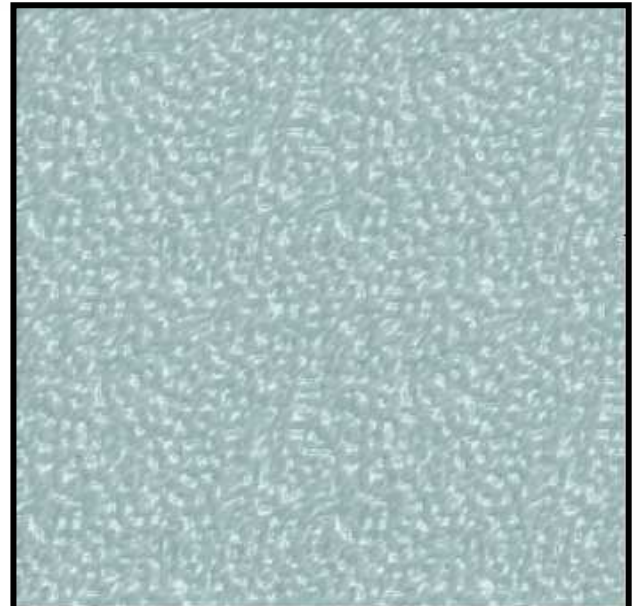
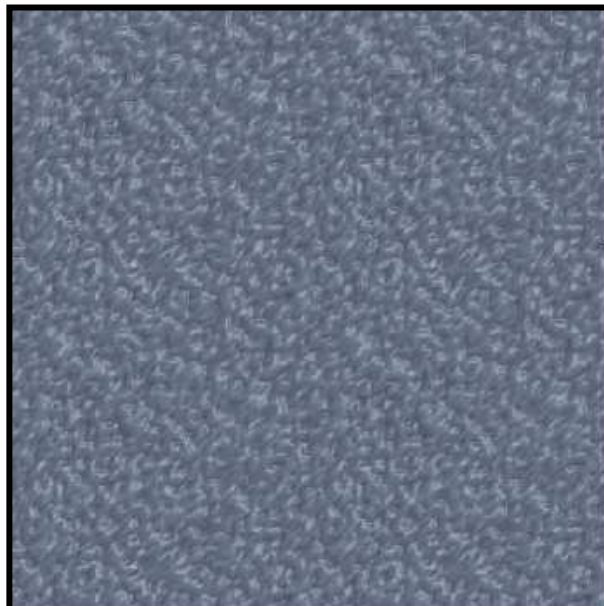
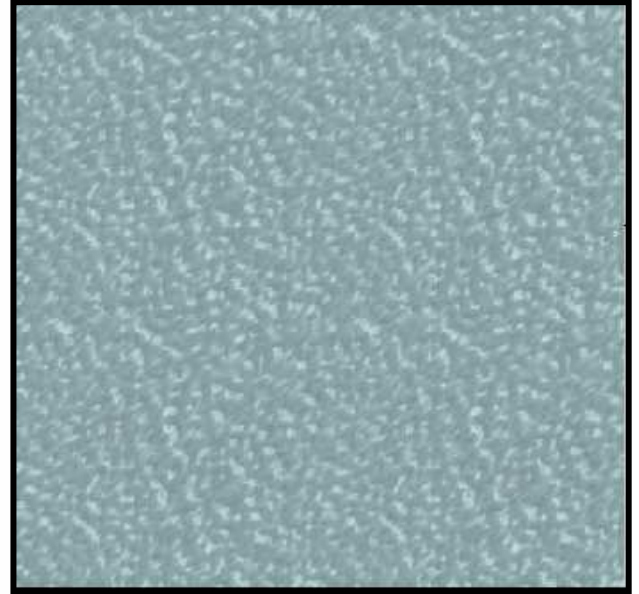
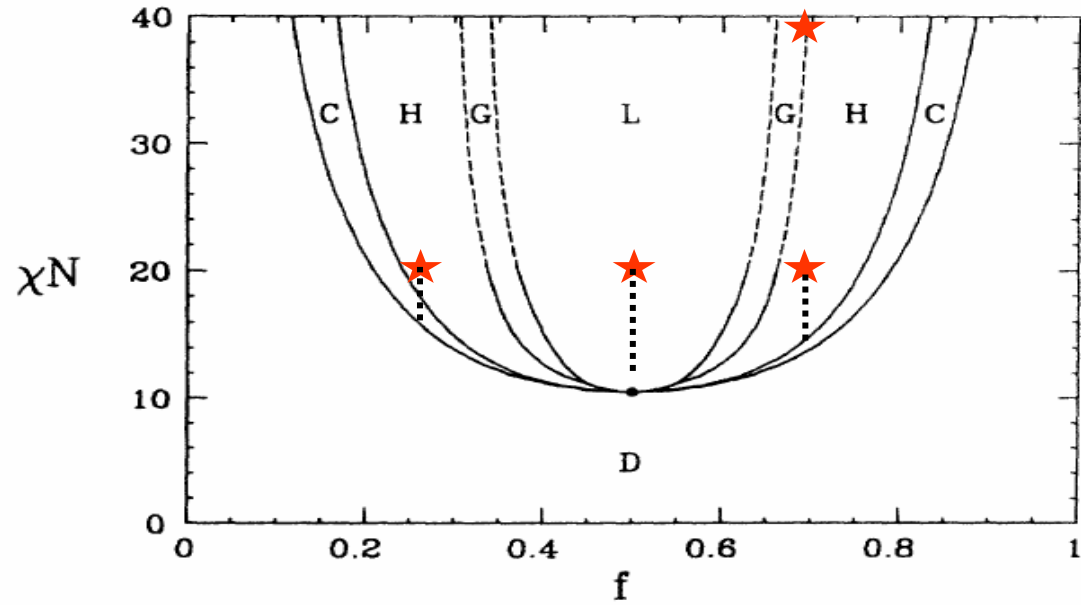


Self Assembled Nanostructure

IBM has trumpeted a nanotech method for making microchip components which it says should enable electronic devices to continue to get smaller and faster. Current techniques use light to help etch tiny circuitry on a chip, but IBM is now using molecules that assemble themselves into even smaller patterns.



Phase Diagram/Structure





Model Structure: Level Set

$$\frac{\partial \Phi}{\partial t} + \mathbf{u} \cdot \nabla \Phi = 0$$

$$\frac{\partial}{\partial t} \rho(\Phi) u_i + \frac{\partial}{\partial x_j} \rho(\Phi) u_i u_j = -\frac{\partial p}{\partial x_i} + \frac{\partial \tau_{ij}}{\partial x_i} + \rho(\Phi) g_i - \sigma K(\Phi) \delta(\Phi) \frac{\partial \Phi}{\partial x_i}$$

$$K(\Phi) = \nabla \cdot \vec{n} \quad \text{and} \quad \vec{n} = \nabla \Phi / |\nabla \Phi|$$

$$\rho(\Phi) = \lambda + (1 - \lambda)H(\Phi) \quad \text{where} \quad \lambda = \rho_1 / \rho_2$$

$$\mu(\Phi) = \eta + (1 - \eta)H(\Phi) \quad \text{where} \quad \eta = \mu_1 / \mu_2$$

$$H = \begin{cases} 0 & \Phi < \varepsilon \\ 1/2 \{1 + \Phi/\varepsilon + \sin(\pi\Phi/\varepsilon)\} & -\varepsilon < \Phi < \varepsilon \\ 1 & \Phi > \varepsilon \end{cases}$$



Model Structure: Level Set

$$\frac{\partial \Phi}{\partial t} + \mathbf{u} \cdot \nabla \Phi = 0$$

$$\frac{\partial}{\partial t} \rho(\Phi) u_i + \frac{\partial}{\partial x_j} \rho(\Phi) u_i u_j = -\frac{\partial p}{\partial x_i} + \frac{\partial \tau_{ij}}{\partial x_i} + \rho(\Phi) g_i - \sigma K(\Phi) \delta(\Phi) \frac{\partial \Phi}{\partial x_i}$$

$$K(\Phi) = \nabla \cdot \vec{n} \quad \text{and} \quad \vec{n} = \nabla \Phi / |\nabla \Phi|$$

$$\rho(\Phi) = \lambda + (1 - \lambda) H(\Phi) \quad \text{where} \quad \lambda = \rho_1 / \rho_2$$

$$\mu(\Phi) = \eta + (1 - \eta) H(\Phi) \quad \text{where} \quad \eta = \mu_1 / \mu_2$$

$$H = \begin{cases} 0 & \Phi < \varepsilon \\ 1/2 \{1 + \Phi/\varepsilon + \sin(\pi\Phi/\varepsilon)\} & -\varepsilon < \Phi < \varepsilon \\ 1 & \Phi > \varepsilon \end{cases}$$



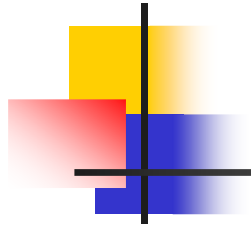
The Level Set Approach

The Level set equation

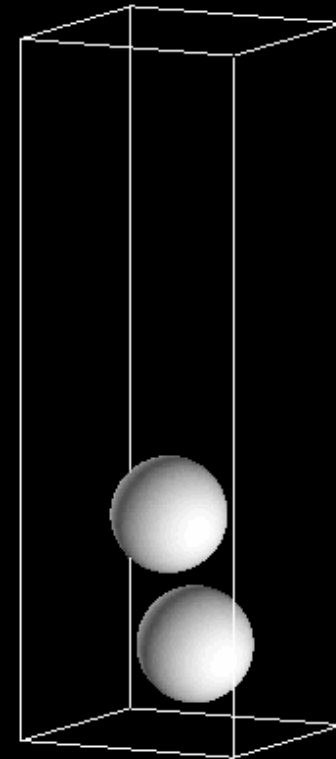
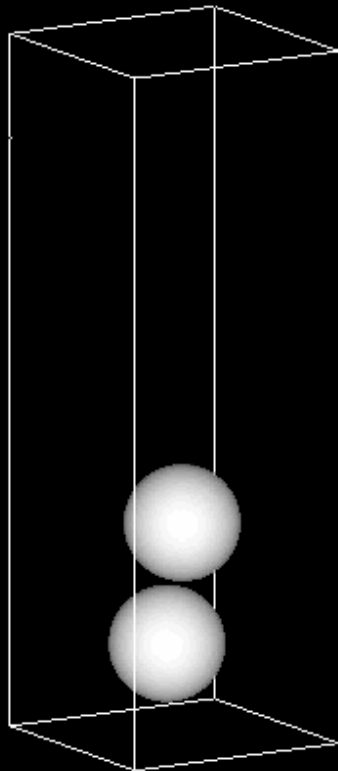
$$\frac{\partial \varphi}{\partial t} + u_j \frac{\partial \varphi}{\partial x_j} = 0.$$

Forcing Φ to be a distance function
(reinitialization)

$$\frac{\partial \varphi}{\partial t} = S(\varphi_0)(1 - |\nabla \varphi|) + \lambda_{i,j,k} f(\varphi_0)$$

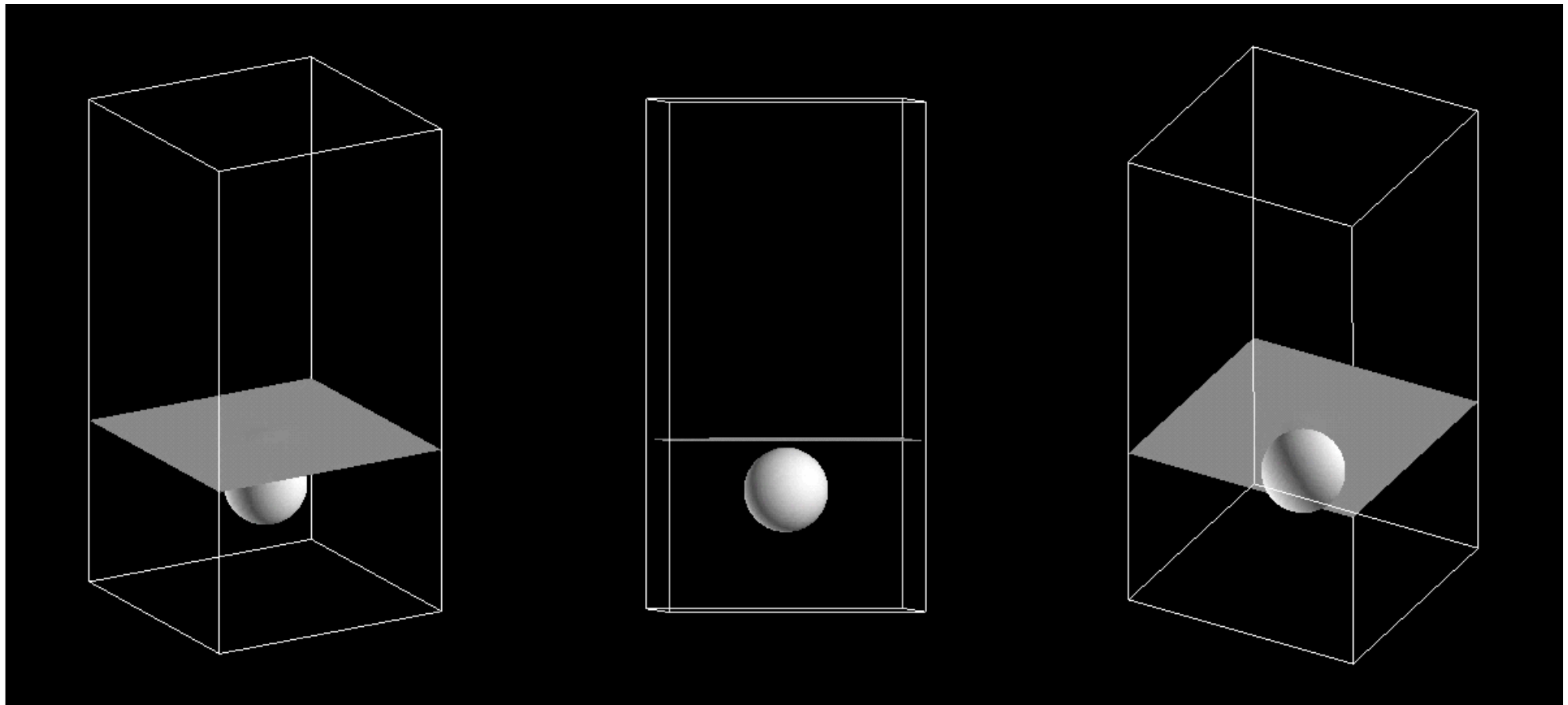


Applications: Bubble Mergers





Applications: Bubble Interface Interaction



Ghost Fluid Method

$$\left[\begin{array}{c} \vec{N} \\ \vec{T}_1 \\ \vec{T}_2 \end{array} \right] (pI - \tau) \vec{N}^T = \begin{pmatrix} \sigma \kappa \\ 0 \\ 0 \end{pmatrix}$$

Sharp treatment of interfacial changes

N – local interface normal

T1/T2 – local interface tangents

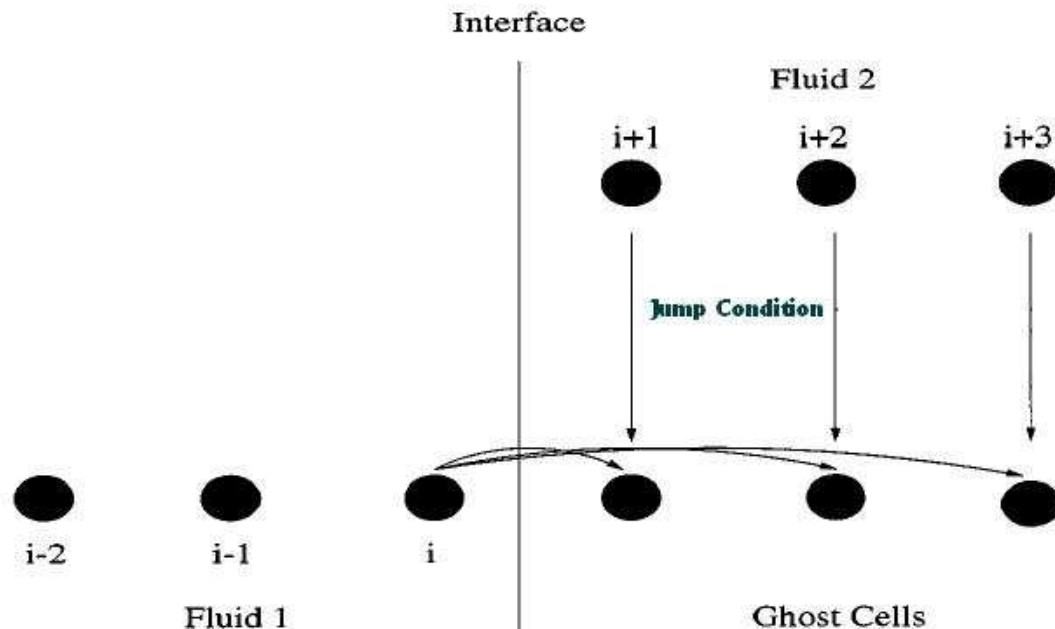
P – pressure tensor

tau – viscous stress tensor

Sigma – surface tension

Kappa – local interface curvature

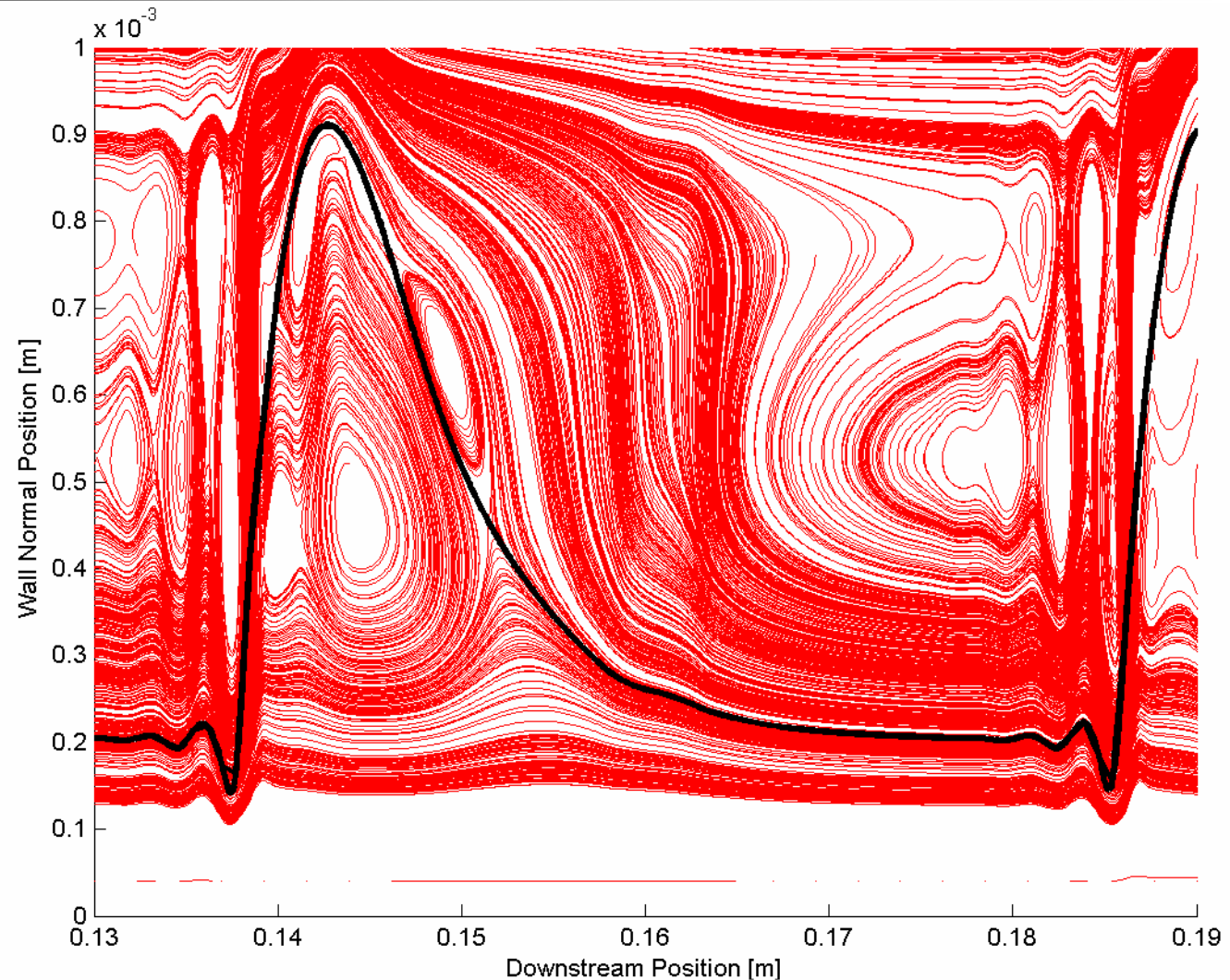
[.] denotes the local interface jump condition



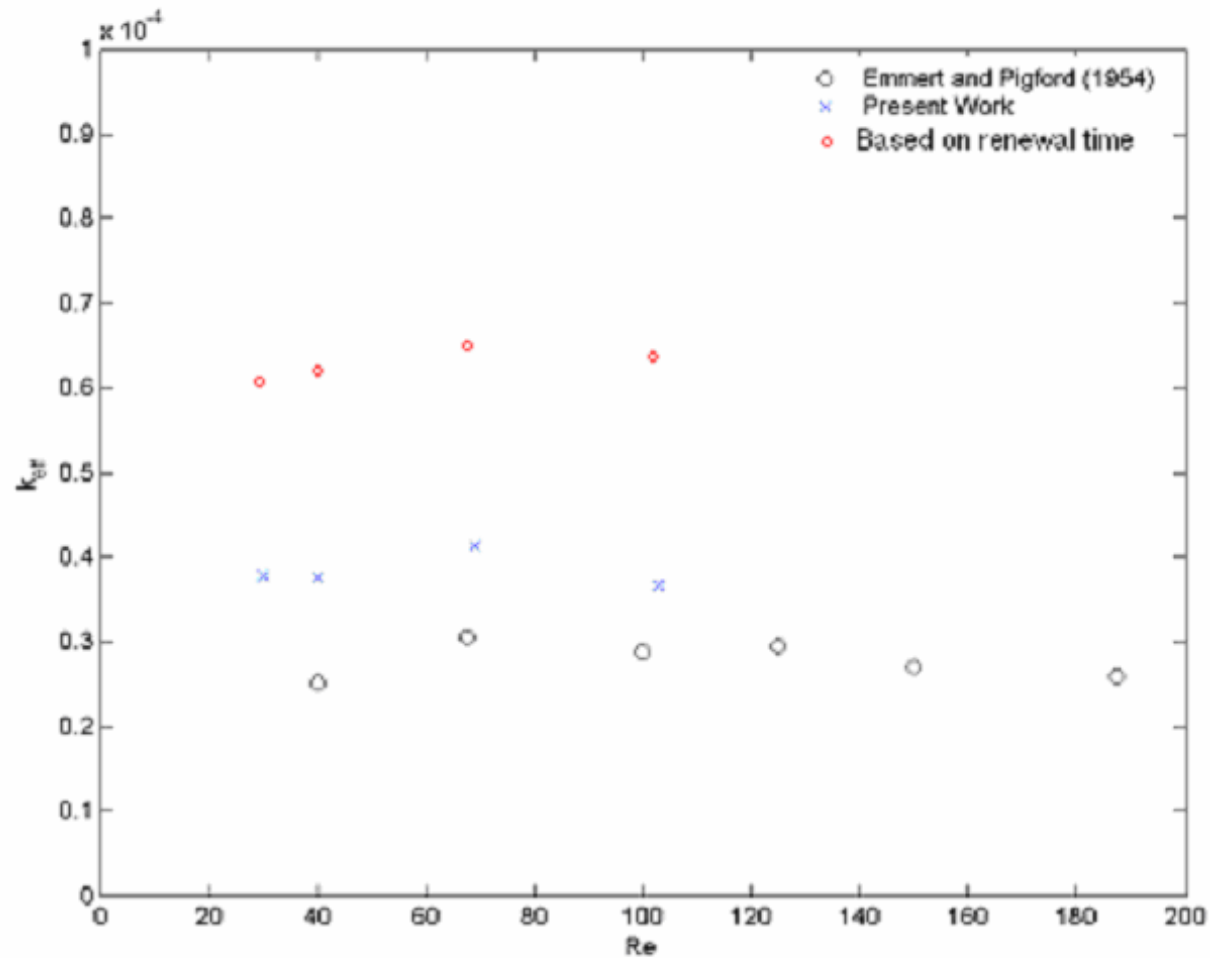
2D Vertical Falling Liquid Films: Analysis of a Wave: Streamlines

Re= 69

We= 0.2785

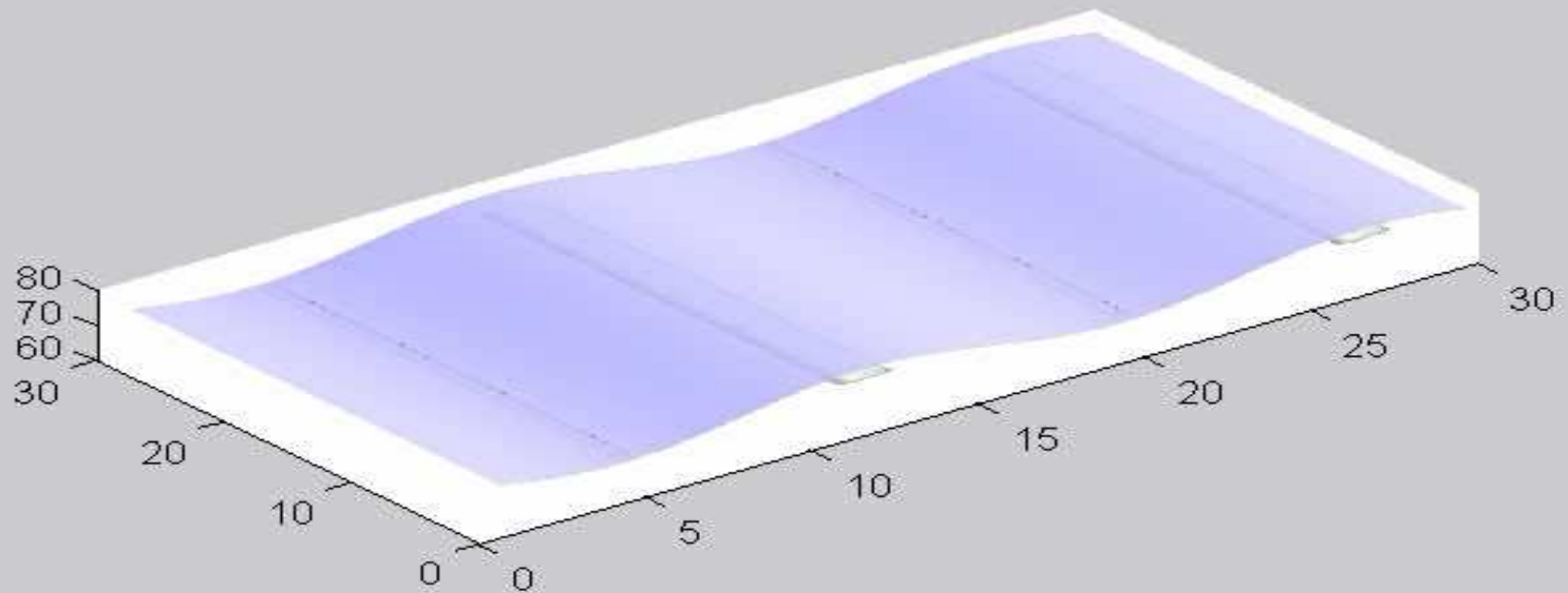


Wave Effects on Interfacial Scalar Transfer



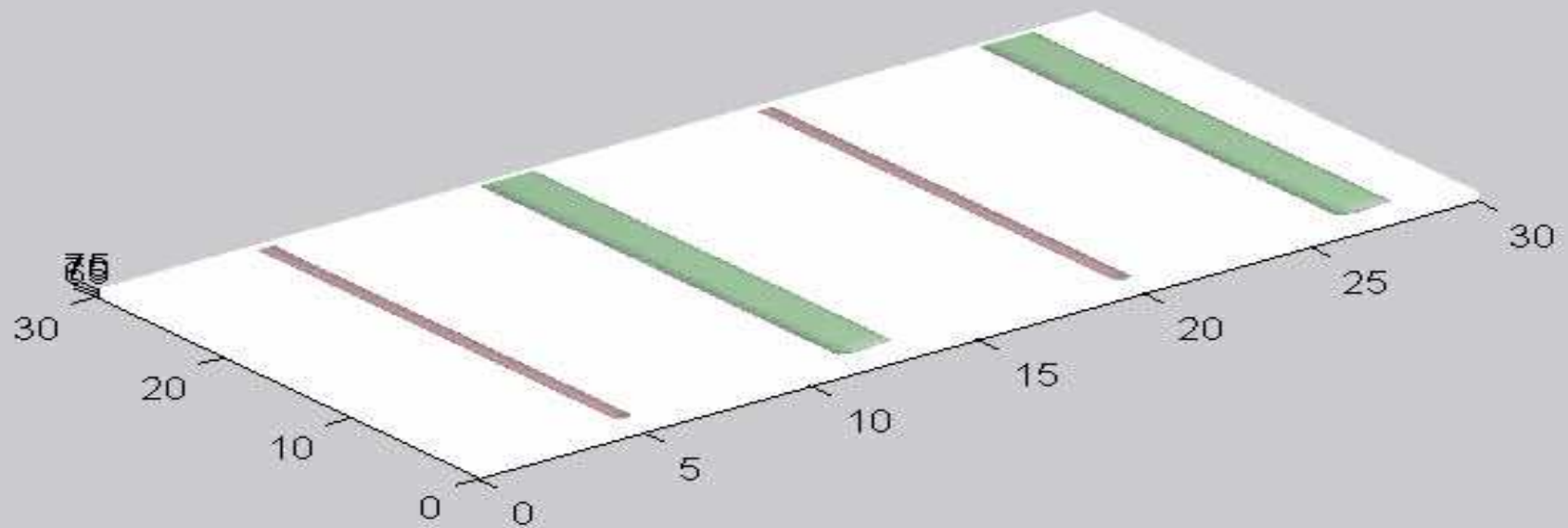


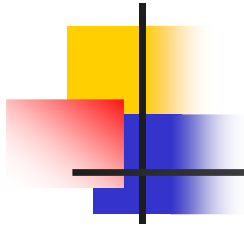
Turbulent Film Flow (Vortices Scaled Up)



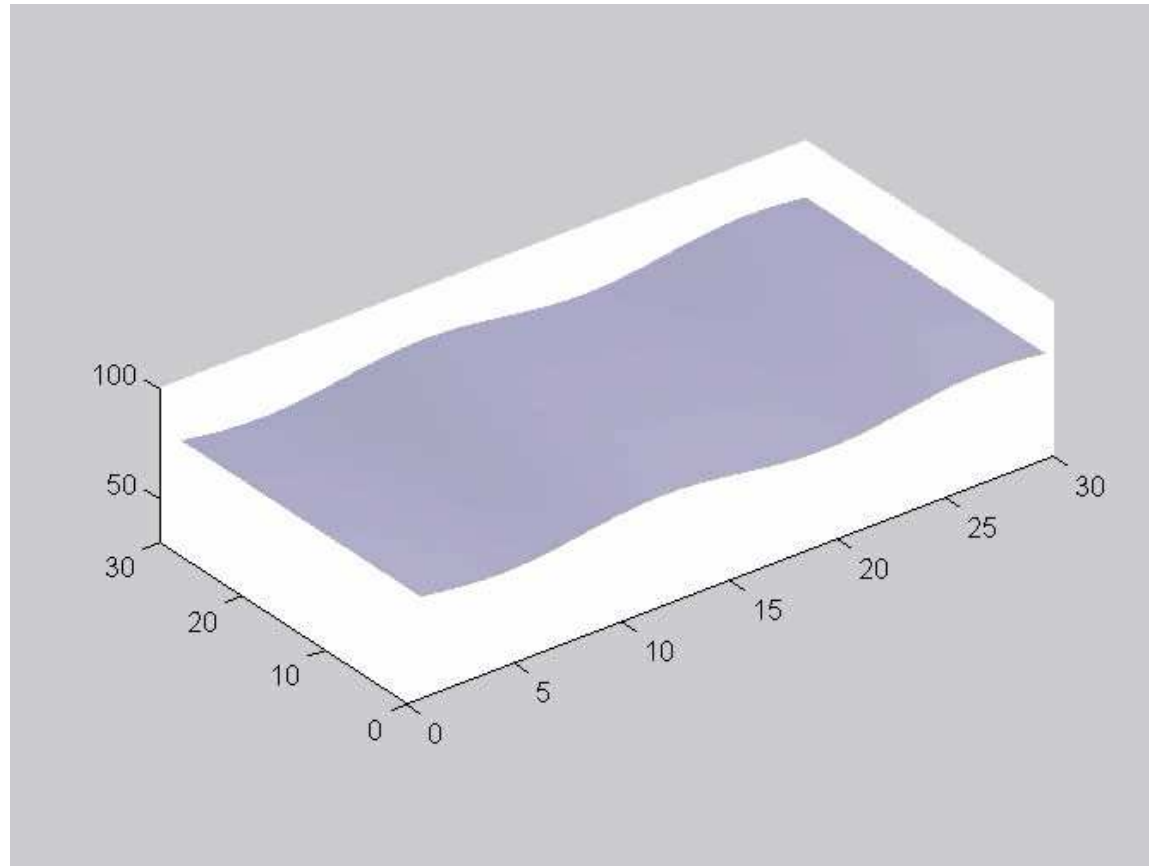


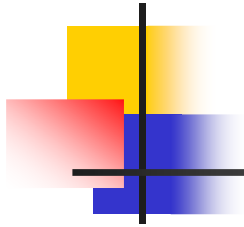
Coherent Structures: Turbulent Film Flow



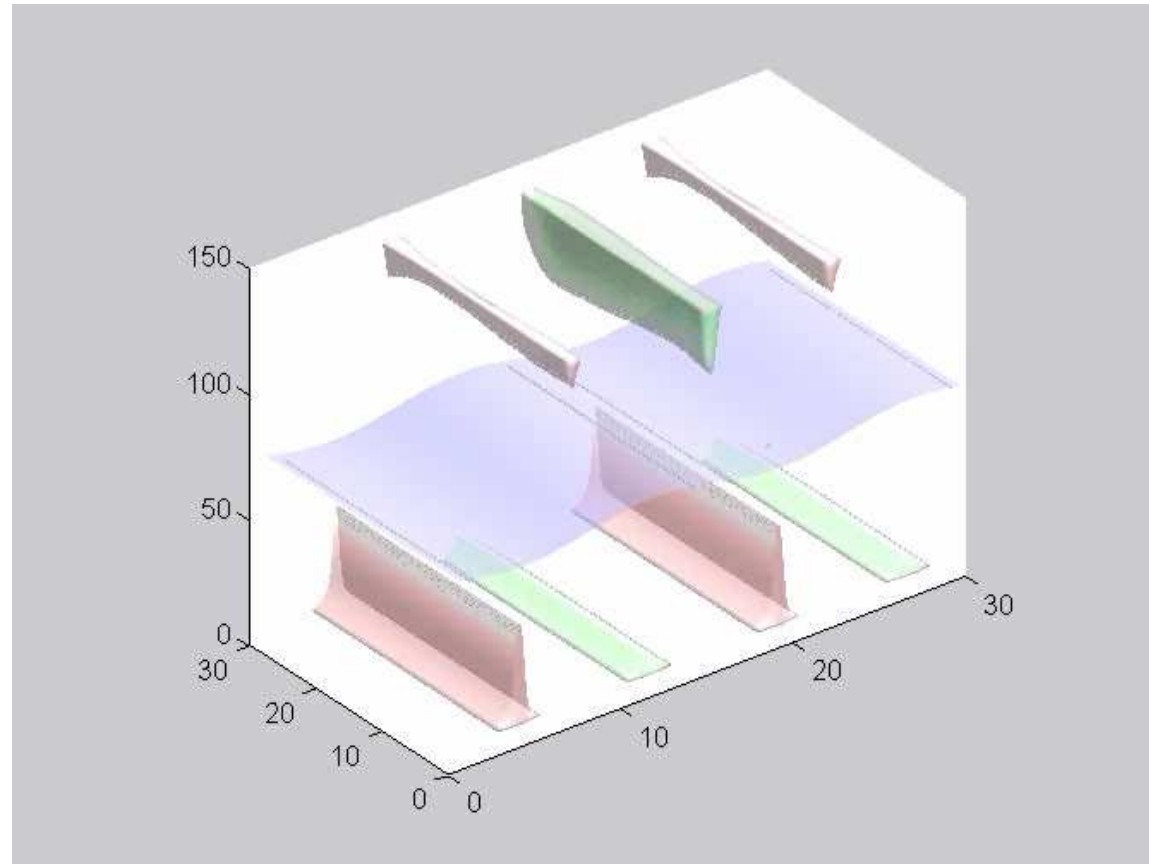


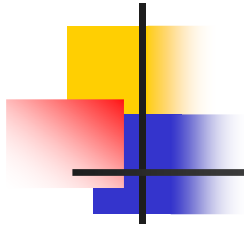
Gas-driven Two-phase Flow



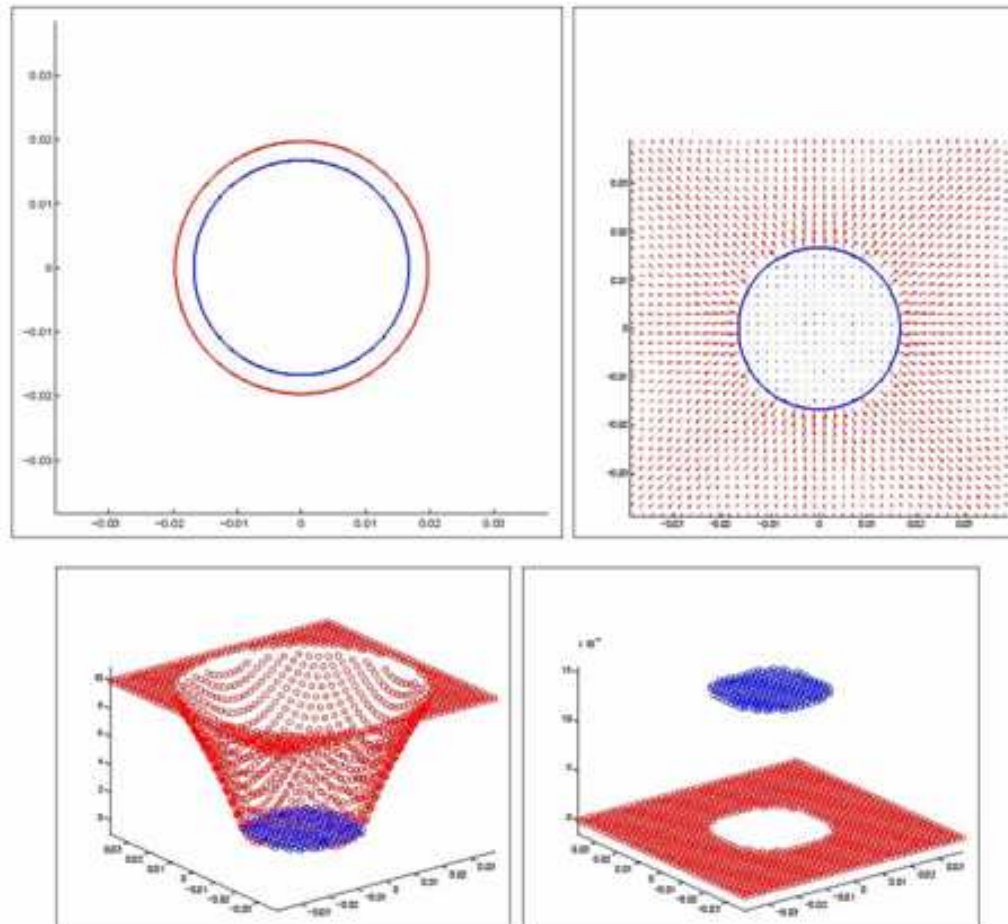


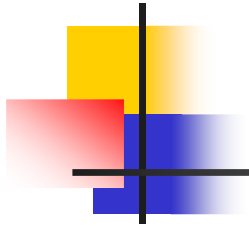
Vortices in gas-driven flow



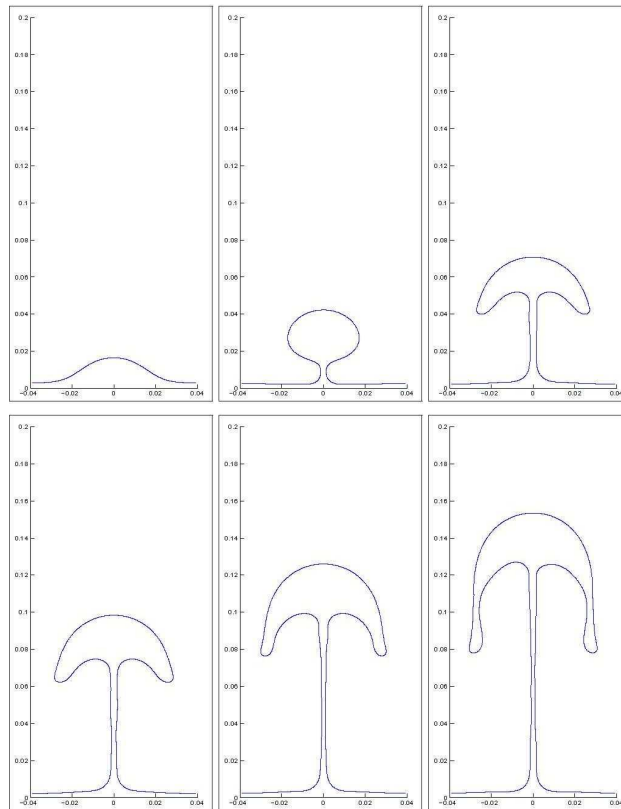


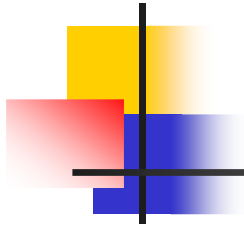
Drop Vaporisation



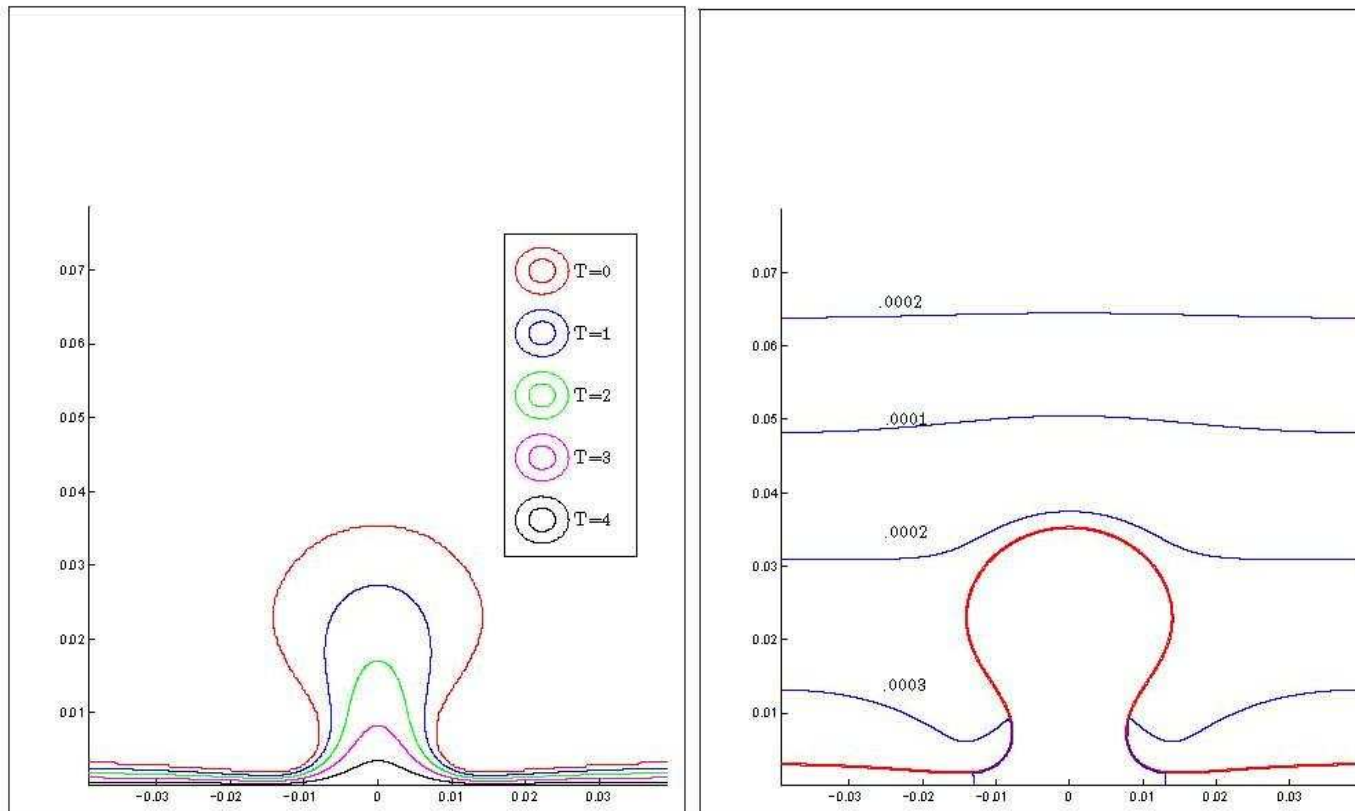


Film Boiling

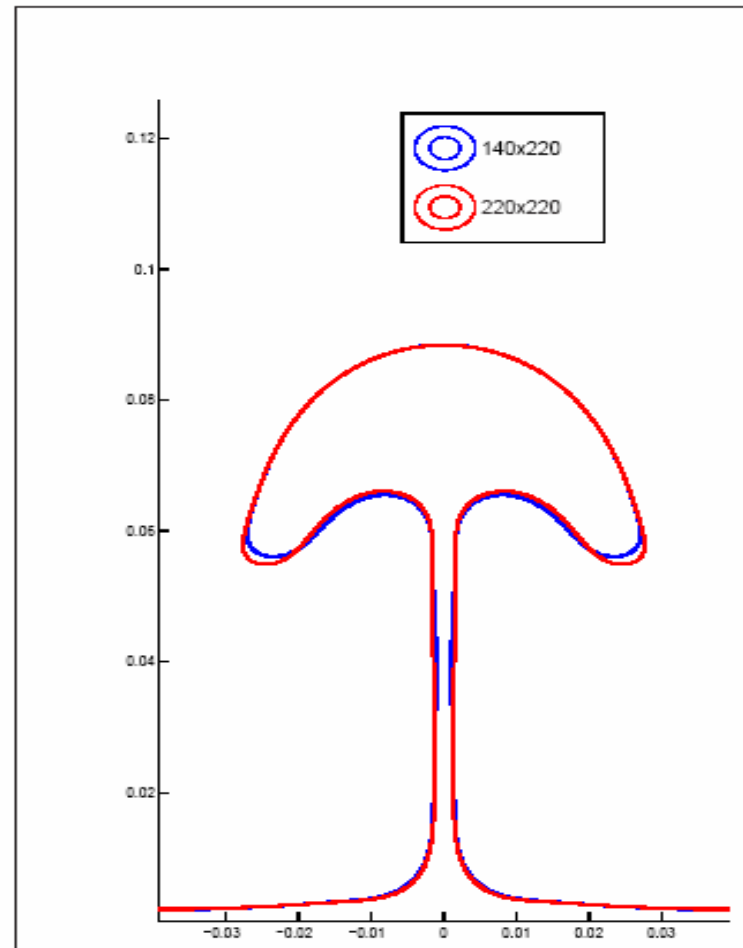




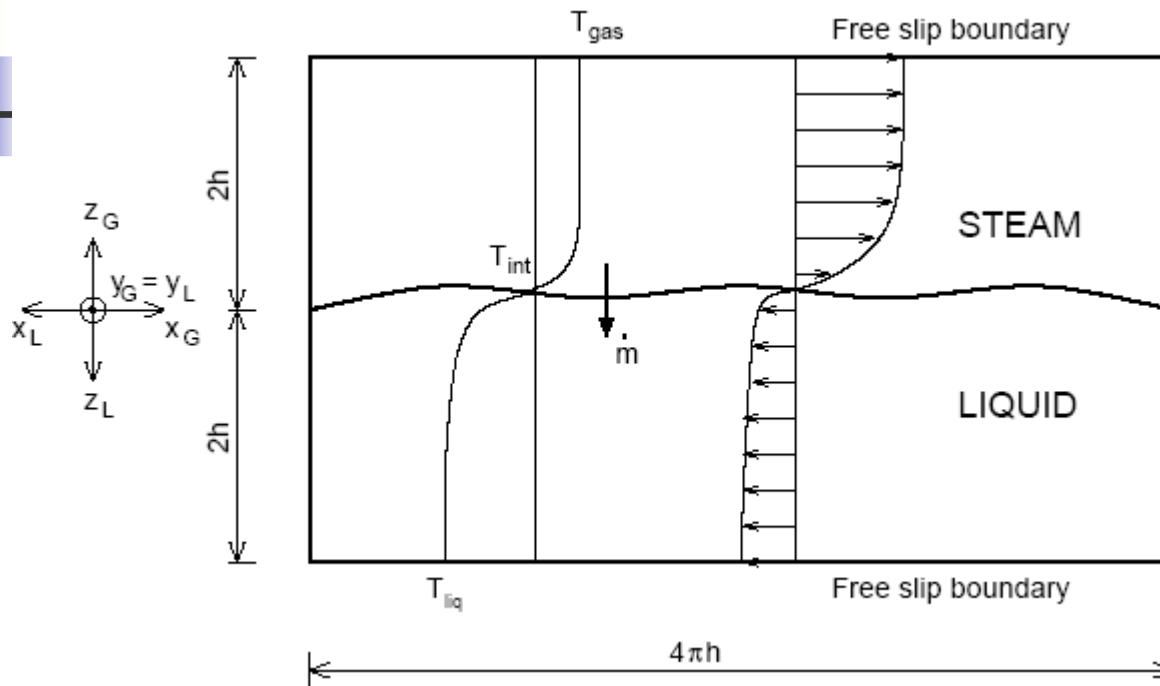
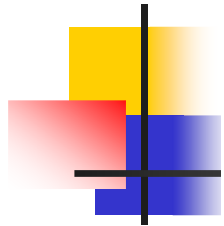
Temperture Contours



Convergence on Mesh Refinement

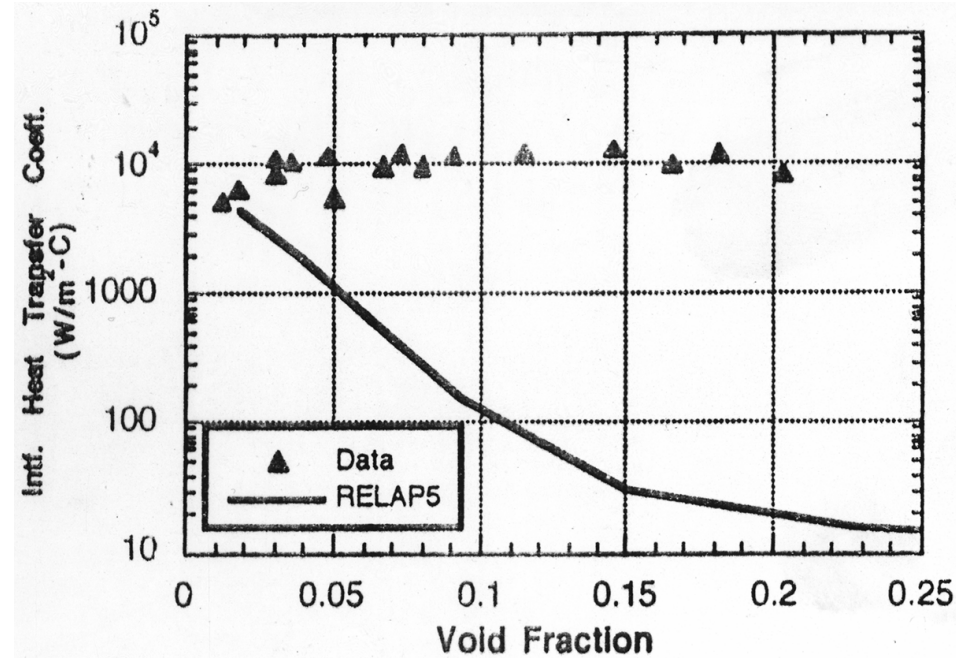


Condensation



- Steam & water cocurrent or countercurrent
- Low steepness wave field ($ak = 0.01-0.17$, capillary/gravity ripples)
- Variable Pr/Sc , shear velocities u^* , and subcooling/superheating

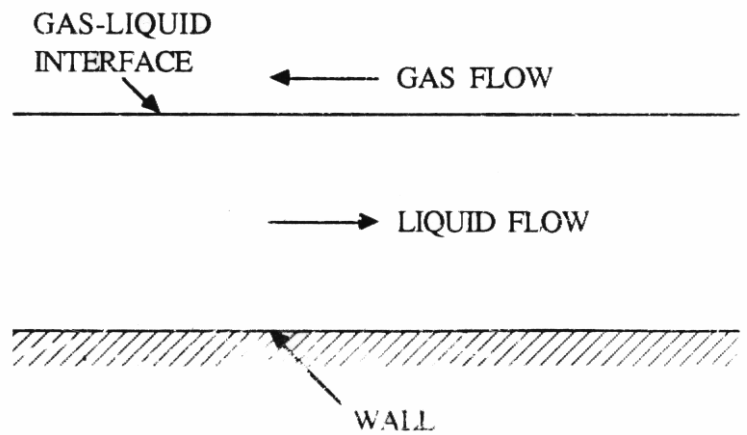
Scalar transfer: sheared interfaces



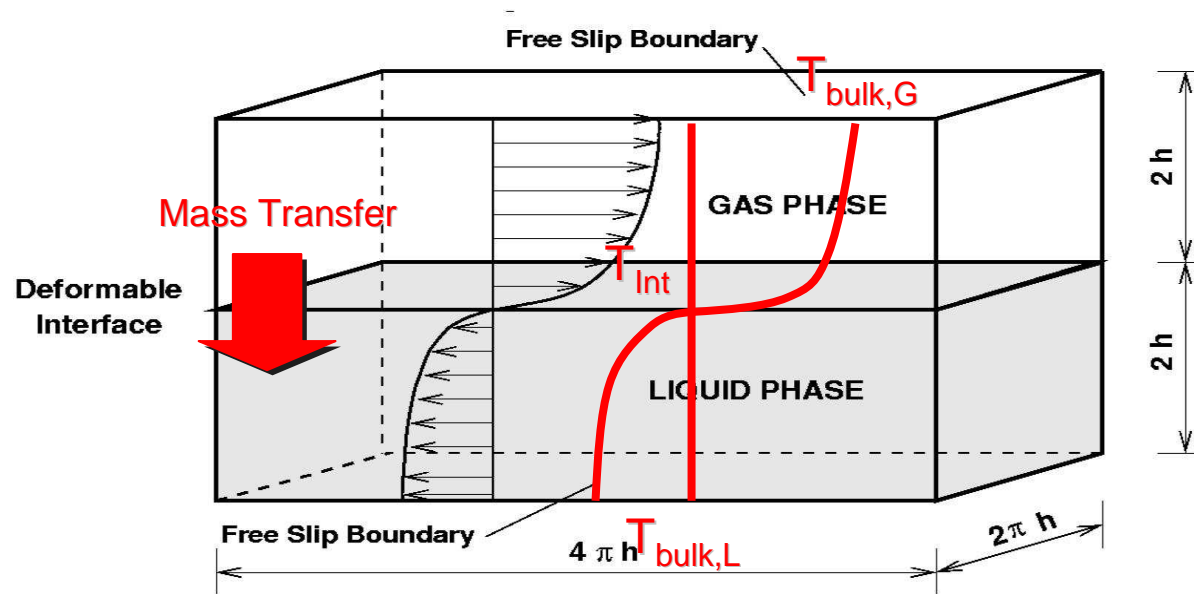
Comparison of RELAP5 predicted values for the interfacial heat transfer coefficient in subcooled boiling vs. McMasters University data



Canonical Problem



DNS Problem Schematic



Fractional time step taken in gas and liquid domains

Finer grid on liquid side for mass transfer calculations



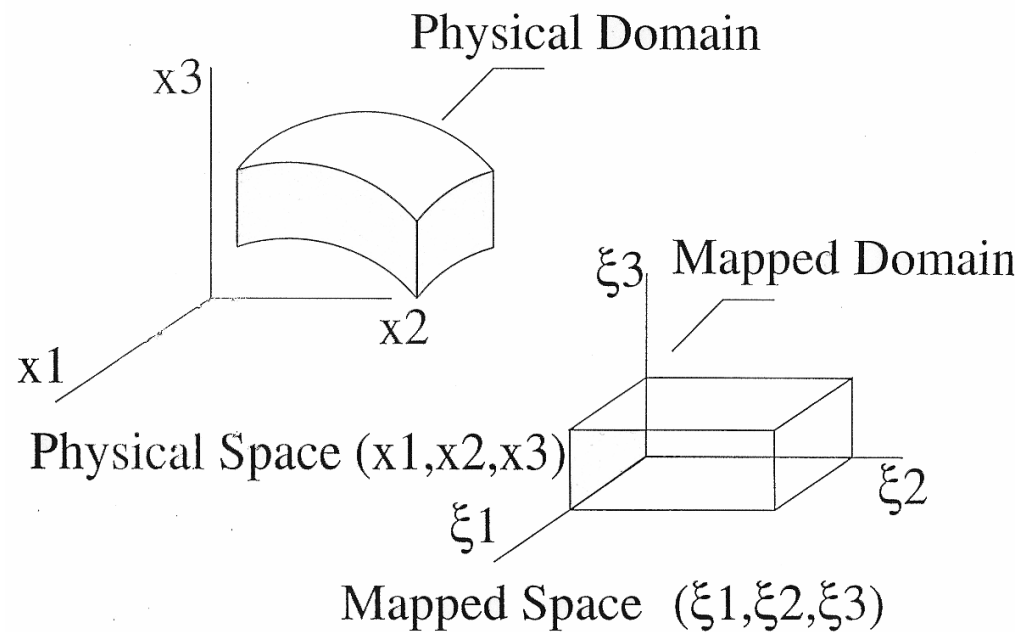
DNS method

- **Pseudo-spectral DNS solver (Fourier-Fourier-Chebyshev).**
- **Uses mapping in the gravity direction (De Angelis, 1998).**
- **Based on a projection method.**
- **Grid resolution: typically 128X128X129 (each domain)**
- **Alternate solution of gas and liquid domains**
- **Fractional steps in each domain: interfacial stress from gas**
- **Interfacial velocity from liquid to gas**



Non-Orthogonal Mapping

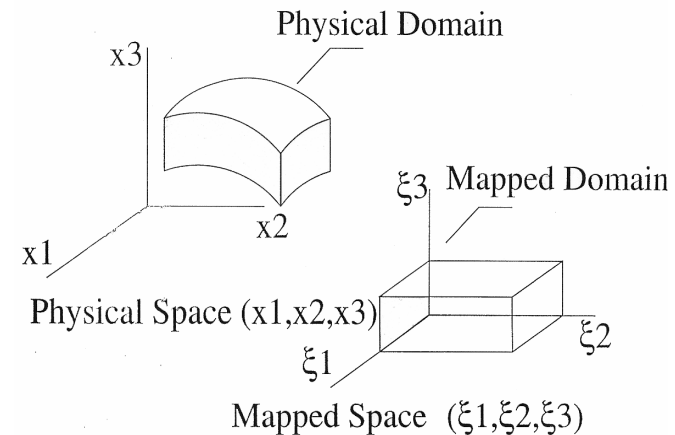
The equations are expressed in new coordinate system.



Boundary Fitting Method

$$\frac{\partial u_i}{\partial t} + u_j \frac{\partial u_i}{\partial x_j} = -\frac{\partial p}{\partial x_i} + \frac{1}{\text{Re}} \frac{\partial^2 u_i}{\partial x_i^2}, \frac{\partial u_j}{\partial x_j}$$

$$\frac{\partial T}{\partial t} + u_j \frac{\partial T}{\partial x_j} = \frac{1}{\text{RePr}} \frac{\partial^2 T}{\partial x_i^2}$$

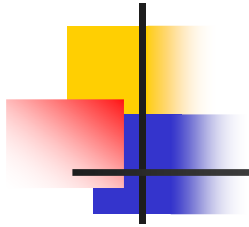


Interfacial jump conditions

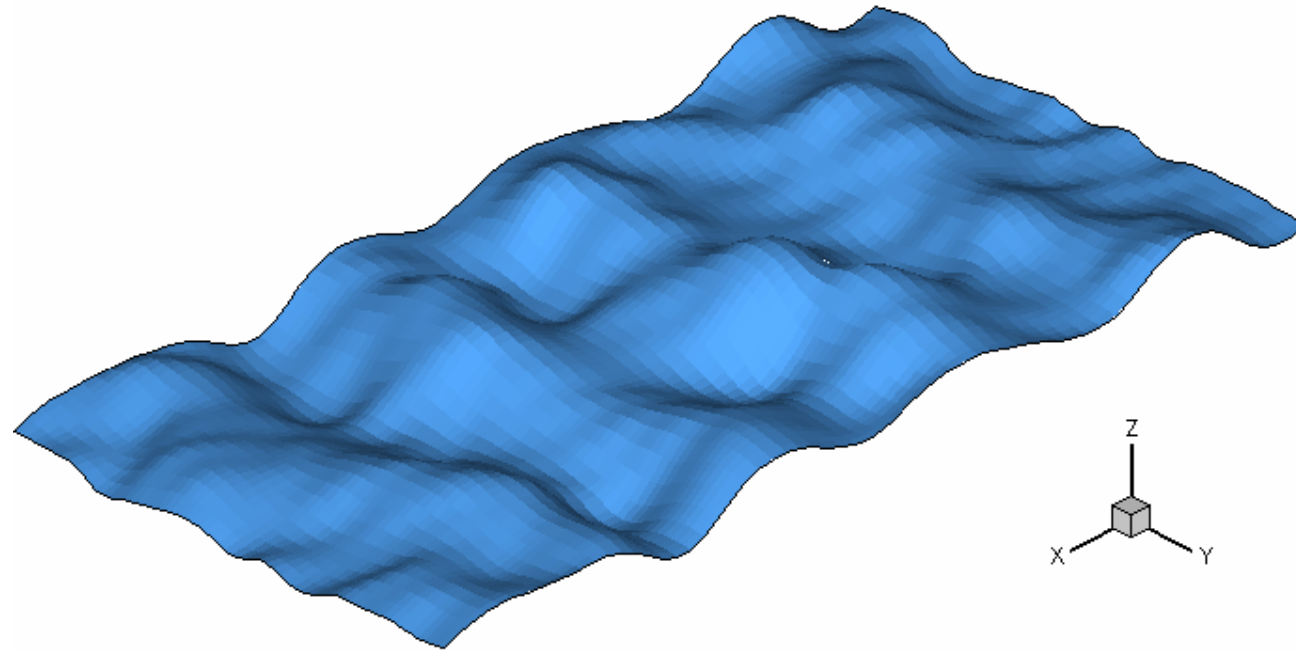
$$\left\{ \begin{array}{l} \frac{1}{\text{Re}} [(\underline{\tau}_L - \underline{\tau}_G) \cdot \underline{n}] \cdot \underline{n} + p_G - p_L - \frac{1}{\text{We}} \nabla \cdot \underline{n} + \frac{1}{\text{Fr}} f = 0 \\ [(\underline{\tau}_L - \underline{\tau}_G) \cdot \underline{n}] \cdot \underline{t}_i = 0 \\ \underline{u}_G = \underline{u}_L \\ T_G = T_L \end{array} \right.$$

$$\frac{\partial f}{\partial t} + u_j \frac{\partial f}{\partial x_j} = 0$$

Interface advection



Interfacial Motion



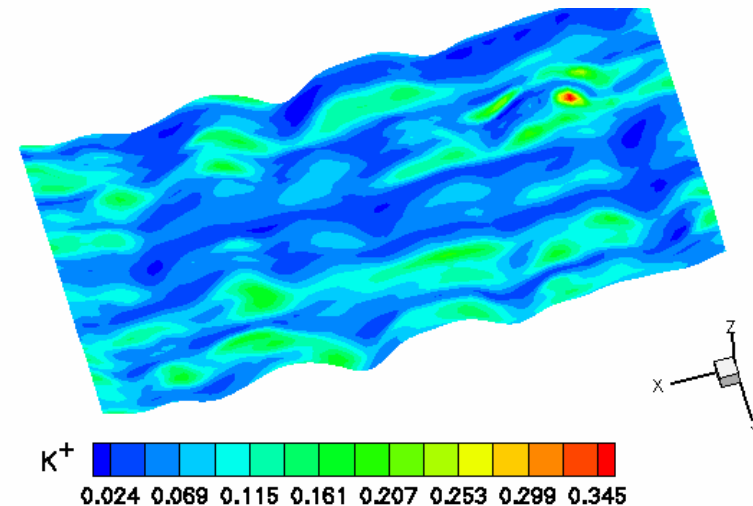
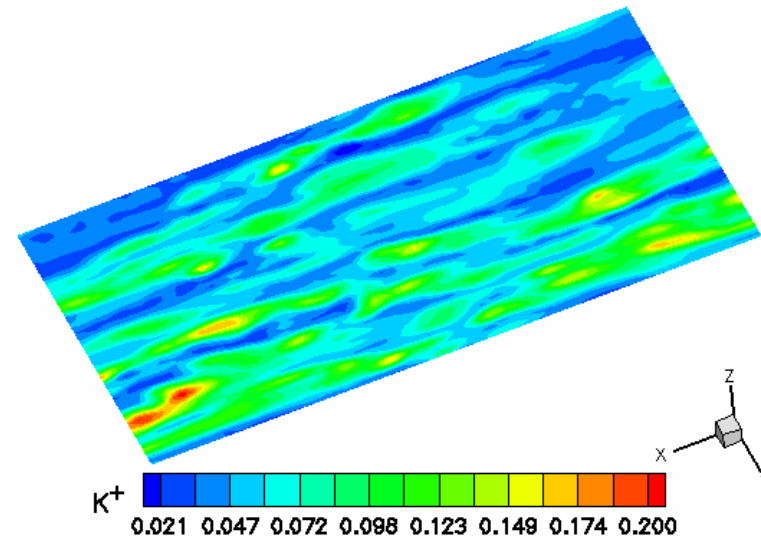
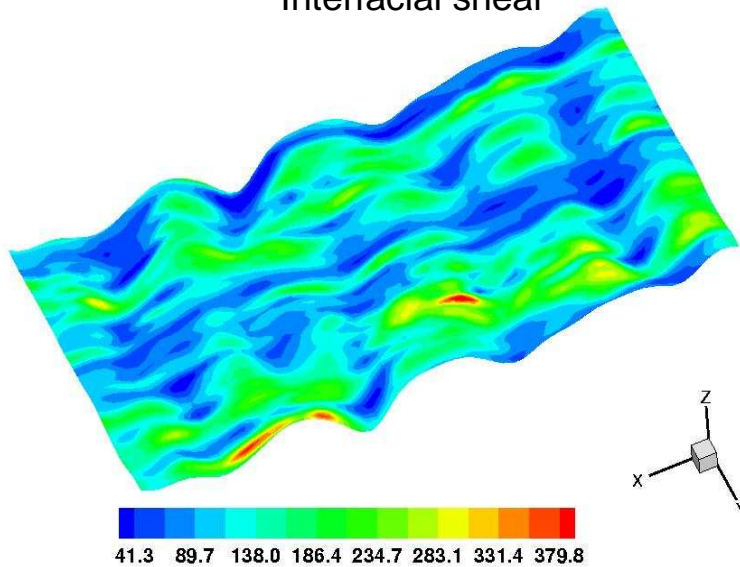
Heat Transfer at the Interface

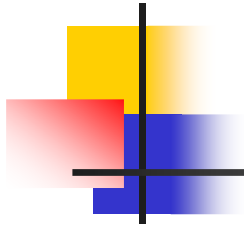
HTC (flat & wavy interface); Pr=1

Interfacial heat transfer

$$K^+ = \frac{q_{\text{int}}}{\rho C_p (\bar{T}_{\text{bulk}} - \bar{T}_{\text{int}}) u_\tau}$$

Interfacial shear

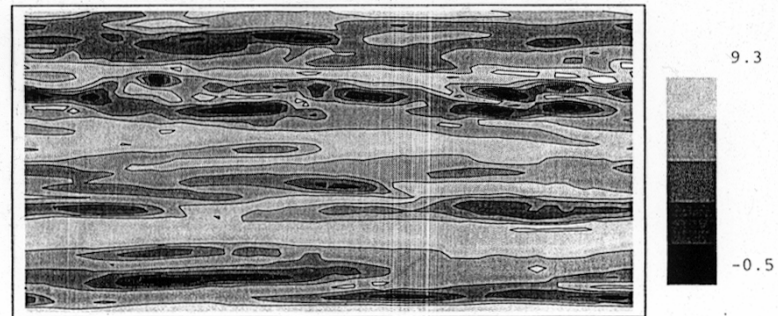




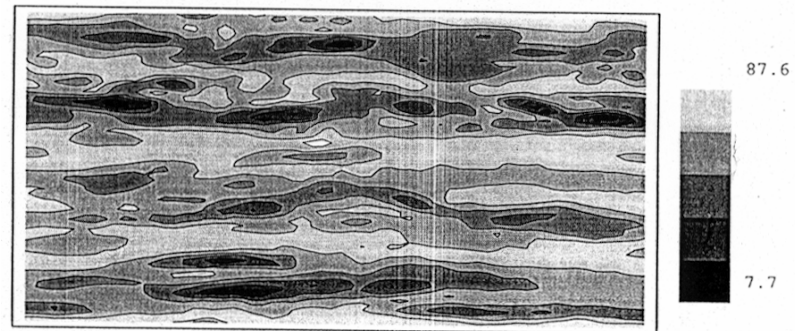
Gas Side Heat Flux vs. Shear Stress

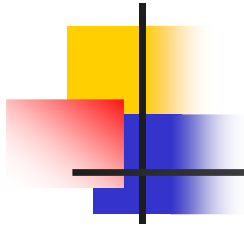
(DeAngelis et al 1997, DeAngelis 1998, DeAngelis et al 2000)

Heat Flux



Shear Stress

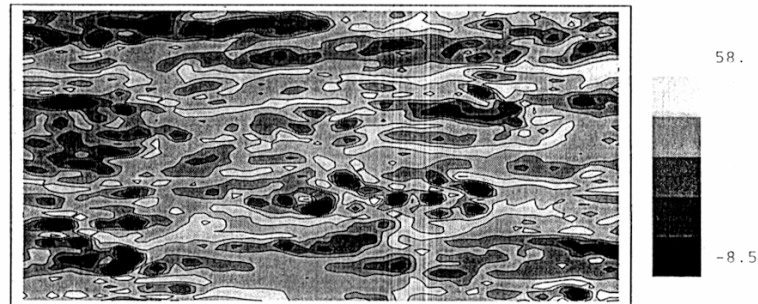




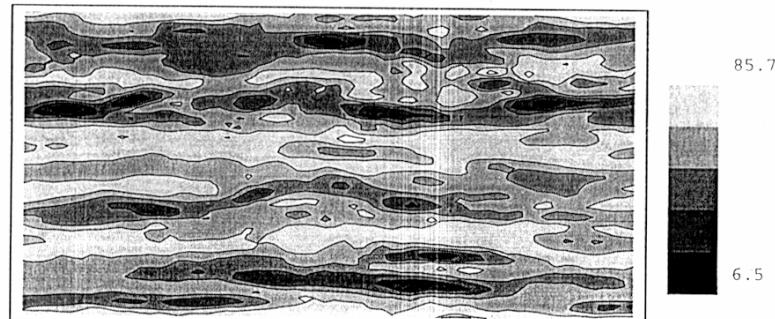
Liquid Side Heat Flux vs. Shear Stress

(DeAngelis et al 1997, DeAngelis 1998, DeAngelis et al 2000)

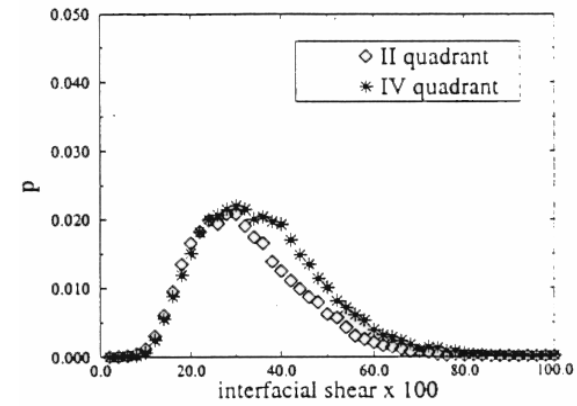
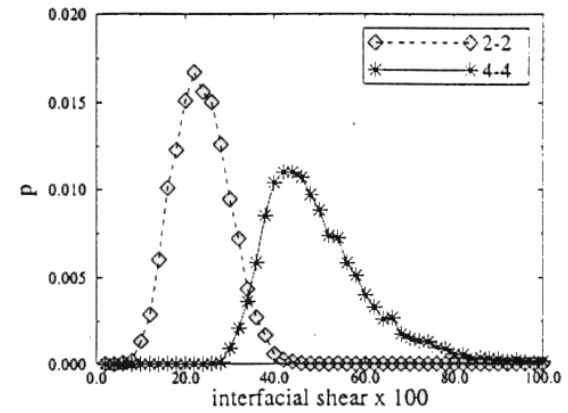
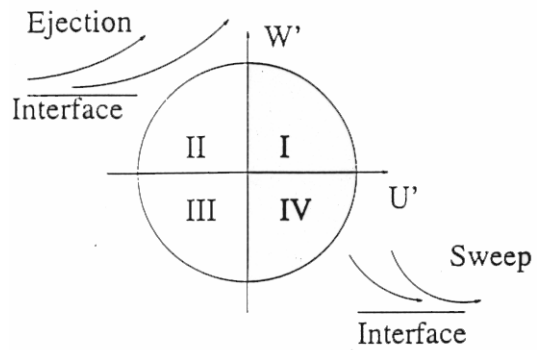
Heat Flux



Shear Stress



Shear stress distribution by quadrant: gas & liquid sides



Surface Renewal Prediction

(Banerjee 1990, DeAngelis et al 1997, DeAngelis 1998, DeAngelis et al 2000)

- Experiment (Rashidi and Banerjee Phys. Fluids **A2** 1827 (1990)) + DNS (Lombardi, De Angelis and Banerjee Phys. Of Fluids **8** 1643 (1996)) suggest:

- Time between burst $t_B^+ = \frac{T_B u_*^2}{\nu} \sim 90$

- Lines between ejections and sweeps: $t_E^+ = \frac{T_E u_*^2}{\nu} \sim 35$

- From surface renewal theory:

- Liquid side: mobile boundary $K_L = \sqrt{D/t_R}$

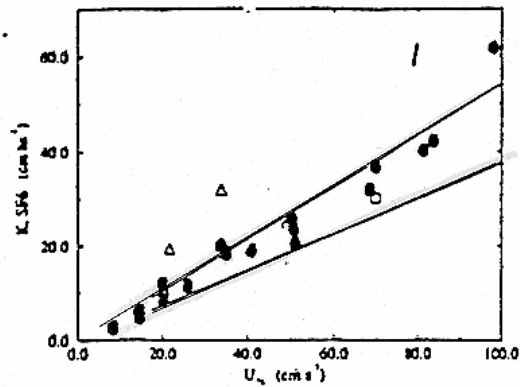
$D \sim$ molecular diffusivity; $t_R \sim$ time between renewals.

- Liquid side: $\frac{K_L Sc_L^{0.5}}{u_{iL}} \sim 0.1$ to 0.15 ; DNS ~ 0.11 ; $u_{iL}^* = \sqrt{\tau_i / \rho L}$

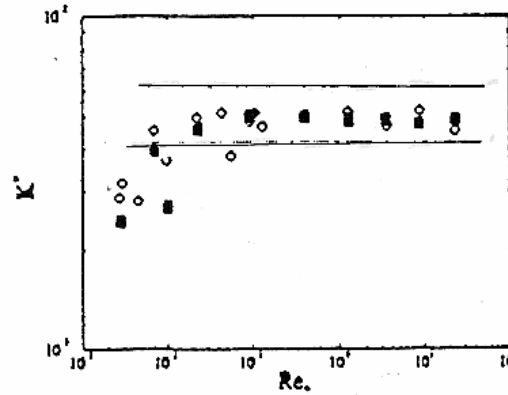
- Gas side: $\frac{K_G Sc_G^{1/3}}{u_{iG}} \sim 0.07$ to 0.09 ; DNS ~ 0.075 ; $u_{iG}^* = \sqrt{\tau_i / \rho G}$

Prediction versus experiment

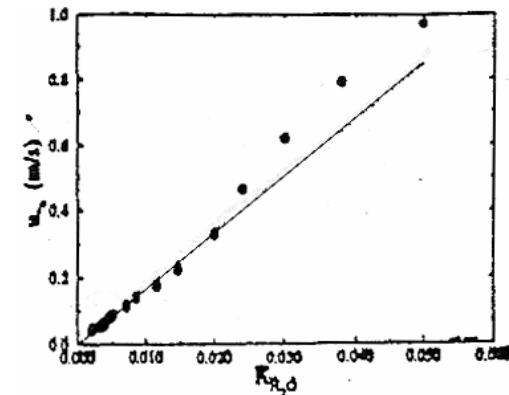
(DeAngelis et al 1997, DeAngelis 1998, DeAngelis et al 2000)



Comparison with the data by Wanninkhof and Bliven (1994). The outlying points are large amplitude waves that were breaking.



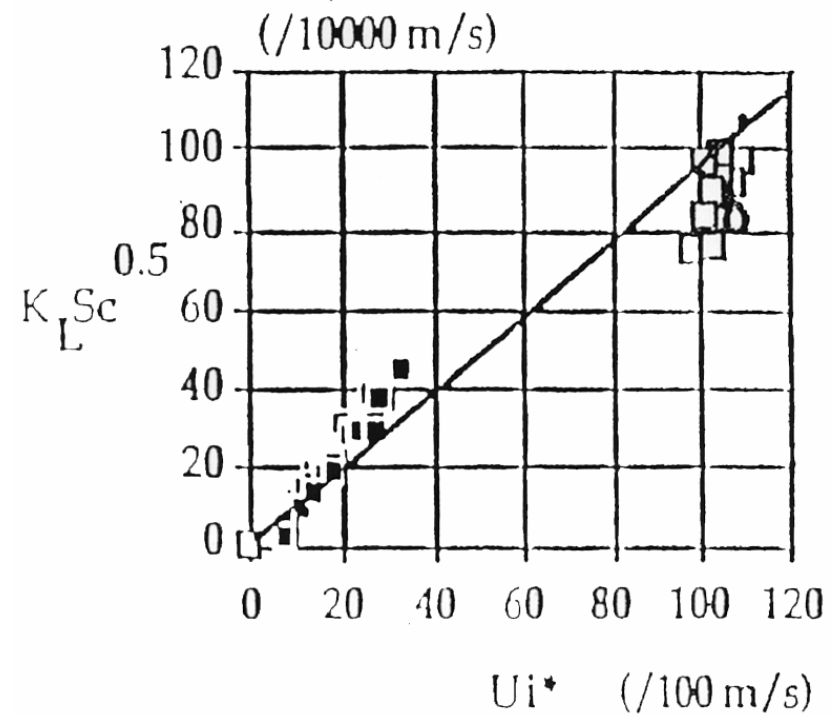
Comparison of Eq. 1 with wind-wave tank gas transfer data from (Ocampo-Torres et al.) Assuming $Sc = 660$.



Comparison of Eq. 2 for moisture flux coefficient with data from Ocampo-Torres et al. (1994)

Bubble column mass transfer

(Cockx et al 1995)



1- Solve Navier Stokes Eqs. in each domain:

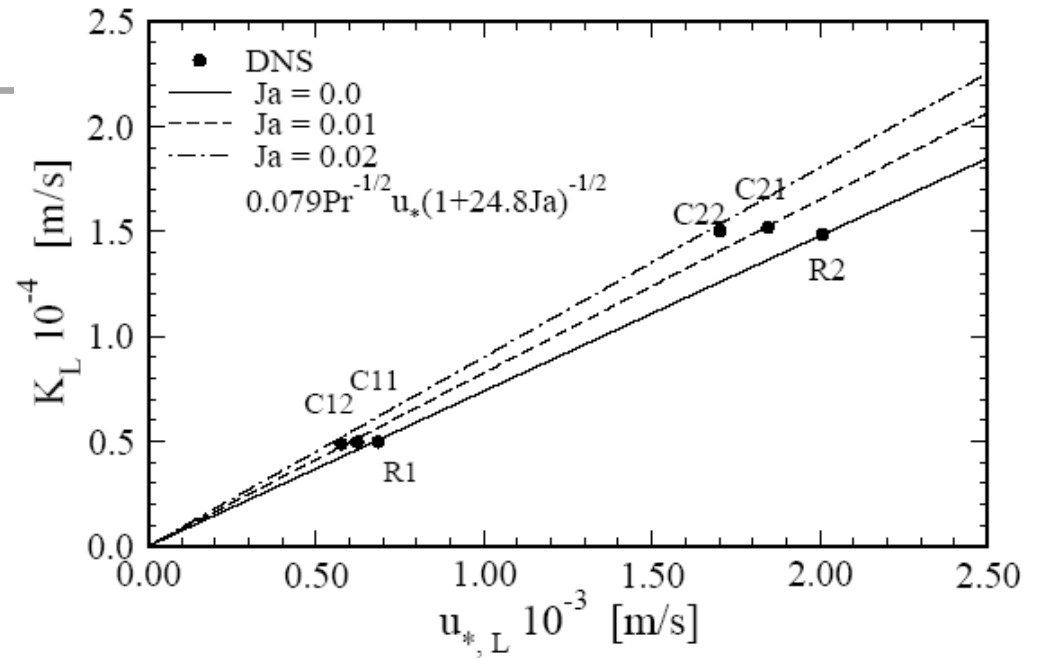
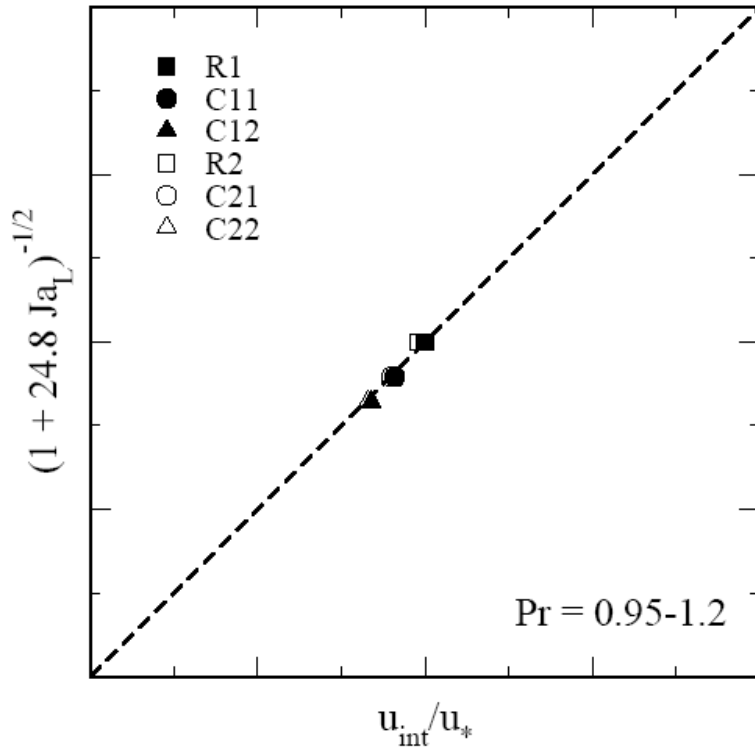
2- Apply Energy jump conditions:

$$\Gamma = \frac{Ja_L}{\text{Re Pr}_L} \nabla T_L \cdot \underline{n} - \frac{Ja_G}{\text{Re Pr}_G} \nabla T_G \cdot \underline{n}$$

$$\left\{ \begin{array}{l} \frac{1}{\text{Re}} [(\underline{\tau}_L - \underline{\tau}_G) \cdot \underline{n}] \cdot \underline{n} + p_G - p_L - \frac{1}{We} \nabla \cdot \underline{n} + \frac{1}{Fr} f + \Gamma^2 (R^2 - 1) = 0 \\ [(\underline{\tau}_L - \underline{\tau}_G) \cdot \underline{n}] \cdot \underline{t}_i = 0 \\ \left(\underline{u}_G - \frac{1}{R} \underline{u}_L \right) \cdot \underline{n} = \Gamma \frac{R^2 - 1}{R} \\ \left(\underline{u}_G - \frac{1}{R} \underline{u}_L \right) \cdot \underline{t}_i = 0 \\ T_G = T_L; R = \sqrt{\rho_L / \rho_G} \end{array} \right.$$

DNS vs. model

$$\frac{u_{\text{int}}}{u_*} = \frac{1}{\sqrt{1 + 24.8\text{Ja}_L}} \quad \text{for } \text{Pr} \sim 1.$$





Conclusions

- Interface capturing models provide a framework that can elucidate many supergird features of two-phase flow structures.
- Fine-scale modeling such as DNS can clarify closure relationships, e.g. for condensation.
- Implicit interface capturing on an Eulerian grid using GFM or phase field is attractive and perhaps can be combined with LBM for bulk fluid computations in future for parralelization.